Magazine of Concrete Research, 2008, **60**, No. 5, June, 313–322
doi: 10.1680/macr.2008.00018

Effect of differential moisture distribution on the shortening of steel-reinforced concrete columns

H. C. Seol*, S.-H. Kwon*, J.-K. Yang†, H.-S. Kim‡ and J.-K. Kim*

Korea Advanced Institute of Science and Technology; Chungwoon University; Konkuk University

This paper presents experimental and analytical studies on the causes of differences between reinforced concrete (RC) and steel-reinforced concrete (SRC) column behaviour with a focus on moisture diffusion. The results of experiments on the long-term behaviour of RC and SRC columns have shown that the shortening of SRC columns tends to be overestimated by the methods generally used to predict the shortening of RC columns. Moisture diffusion coefficient and surface factor of the concrete used in the SRC column specimens were determined from experiments and an analysis on moisture diffusion was conducted to determine the progress of moisture diffusion in the SRC column specimens. The analytical results indicated that the progress of moisture diffusion in SRC columns is quite different from that in RC columns. Analyses on differential drying shrinkage and differential drying creep were also performed by analysing the progress of moisture diffusion at each point in an SRC column section. The results indicated that obstruction of the moisture diffusion route causes a reduction in both drying shrinkage and drying creep in the SRC columns. The differential moisture distribution should therefore be taken into account in order accurately to predict SRC column shortening.

Notation

A_c	cross-section
D_1	maximum of $D(H)$ for $H = 1$
$D(H)$	diffusion coefficient
$\boldsymbol{EA}$	stiffness of a steel section
$E_c(t)$	modulus of elasticity
f	surface factor
$\boldsymbol{f}'_c$	specified compressive strength of concrete
H	relative pore humidity
$\overline{H}$	microdiffusion flux
h	notional size of member
r	a constant for shrinkage
$sign(\overline{H})$	sign of the microdiffusion flux, $\overline{H}$
t	age of concrete
t_0	age of concrete at loading
t_s	age of concrete at the beginning of shrinkage
u	perimeter of the member in contact with the atmosphere
v/s	volume/surface area
w	unit weight of concrete
$\beta_c(t - t_0)$	coefficient to describe the development of creep with time
$\beta_s(t - t_s)$	coefficient to describe the development of shrinkage with time
ΔH	variation of relative humidity
ε_{cso}	notional shrinkage coefficient
ε_s^0	magnitude of the final shrinkage value
$\boldsymbol{\sigma}$	stress in a cross-section
ϕ_0	notional creep coefficient

* Department of Civil and Environmental Engineering, Korea Advanced Institute of Science and Technology, Guseong 373-1, Yuseong, Daejeon, Korea
† Department of Civil and Environmental Engineering, Chungwoon University, Hongseong-eup, Hongseong-gun, Chungnam, Korea
‡ College of architecture, Konkuk University, 1 Hwayang-dong, Gwangjin-Gu, Seoul, Korea

(MACR-D-08-00018) Paper received 8 June 2006; last revised 2 March 2007; accepted 26 March 2007

Introduction

Creep and shrinkage of concrete produce long-term deformations that can cause shortening of vertical elements such as walls and columns in concrete and in composite structures.[1] For columns, this effect—known as 'column shortening'—may lead to undesirable pro-

www.concrete-research.com 1751-763X (Online) 0024-9831 (Print)

blems related to serviceability and structural safety. In particular, differential column shortening, caused by different loads applied to columns and differences in sectional capacities for loading, may deteriorate serviceability by damaging claddings, partitions and equipment.[2] Differential column shortening may also cause additional stress both in beams and in slabs or may produce excessive stress from lateral resistance systems, thus lowering structural safety. With consideration of the ongoing construction of taller buildings, it is becoming increasingly important to be able to predict column shortening accurately.

With the rapid increase of high-rise building construction in recent years, steel-reinforced concrete (SRC) columns have come into wider use, because their sectional efficiency is higher than that of reinforced concrete (RC) columns. The latest experimental study[3] has shown, however, that SRC column shortening tends to be overestimated by the estimation methods generally used to predict the shortening of RC columns. In the case of SRC columns, additional cracks occur at the outer concrete residing just beside the steel section. These phenomena cannot be explained effectively by the existing analysis methods. A new analysis method that incorporates the moisture diffusion properties of SRC columns is therefore required.

In the present paper, the causes of the difference between RC and SRC column behaviour are investigated, with a focus on the moisture diffusion in SRC columns. Analyses on differential drying shrinkage and differential drying creep are also performed through investigation of the progress of moisture diffusion at each point of an SRC column section.

The progress of moisture diffusion in SRC columns is quite different from that in RC columns, because a steel section, such as an H-shaped steel section, obstructs the moisture diffusion route of the inner concrete, as shown in Fig. 1. Consequently, obstruction of the moisture diffusion route causes a reduction of both drying shrinkage and drying creep in SRC columns.[4]

From the results obtained in this study, the shrinkage and creep equations in the Comité Euro-International du Béton–Fédération Internationale de la Précontrainte (CEB–FIP) model code have been accordingly modified in order to predict the shortening of SRC columns more accurately.[5]

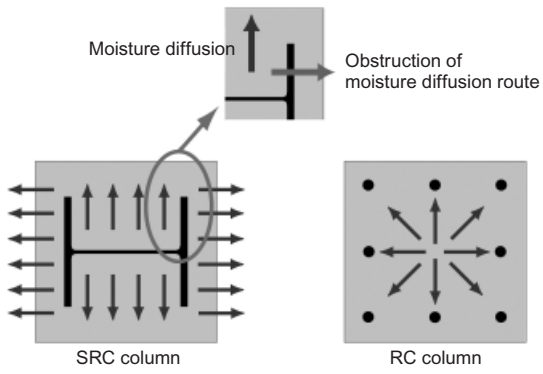

Fig. 1. Obstruction of the moisture diffusion route in SRC columns

Experimental programme

Drying creep and shrinkage of column specimens

Test variables. The test was performed on the basis of the construction data from a specific building under construction ('Yeoeuido Richencia', residential/commercial complex, constructed by Kumho E&C). Fig. 2 shows the dimensions of RC column and SRC column specimens having the same cross-section (150×150 mm^2) and same length (600 mm) but having four different steel ratios of 3·65, 5·48, 6·14 and 9·14% for RC1, SRC1, RC2 and SRC2, respectively. Steel ratios for the specimens were determined from the values that were frequently used in the actual construction data. Two companion specimens for each test variable were manufactured and tested.[3]

Figure 3 shows the dimensions of the control test specimens.[3] Control tests were performed to determine the notional shrinkage coefficient ε_{cso} and the notional creep coefficient ϕ_0 of the inner concrete of column specimens, which are the factors related to the shrinkage and the creep property in the CEB–FIP model code,[6] respectively. The magnitude of the final shrinkage value, ε_s^0, related to the variation of differential drying shrinkage, and a constant for shrinkage, r, related to the variation of stress-induced shrinkage, were also determined from control tests.[4] Two companion specimens for each test variable were manufactured and tested.

Test set-up. Embedment gauges were located at the centre of each column specimen and control specimen for drying creep and shrinkage so as to measure the concrete strains. A spring-loaded frame was used both for column specimens and drying creep control specimens in order to perform the tests under sustained loads over time. All the specimens were tested under conditions of $20 \pm 1°$ and $60 \pm 2\%$ relative humidity (RH).

Two different kinds of load were applied to the column specimens and control specimens for drying creep. RC1, SRC1, SRC2 and control specimens for drying creep were loaded with 250 kN while RC2 was loaded with 280 kN. The age of concrete at initial loading was 28 days and the load was sustained for 60 days.[3]

Mix proportion and material properties. Table 1 shows the two different mix proportions, C1 and C2, for both the RC column specimens and the SRC column specimens, respectively. Mix proportions for the specimens were determined from the values that

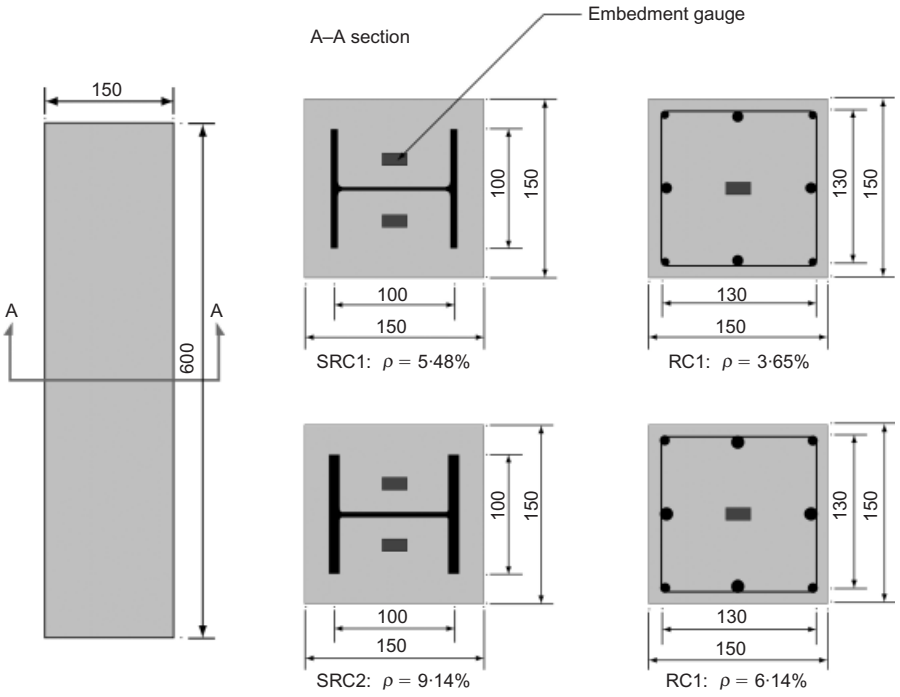

Fig. 2. Dimensions and instrumentation of column specimens. Units: mm

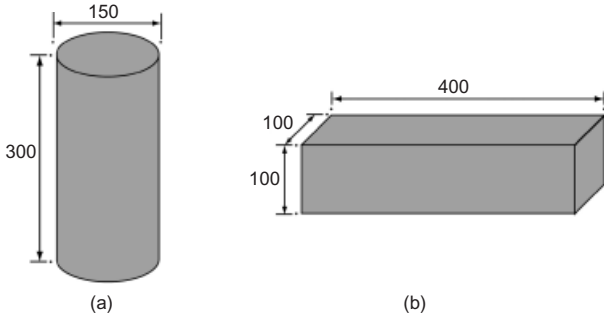

Fig. 3. Dimensions of control specimens: (a) specimen for drying creep; (b) specimen for drying shrinkage. Units: mm

were frequently used in the actual construction data. The same mix proportions, C1 and C2, were also applied to the control test specimens. The maximum aggregate size was 19 mm and type I cement was used in the concrete mix. Table 2 shows the mechanical properties of C1 and C2 concrete.[3]

Table 2. Mechanical properties of concrete

Test variables	Age: days	Elastic modulus: GPa	Strength: MPa
C1 (RC)	28	20·3	31·6
C2 (SRC)	28	24·0	43·0

Experiment on moisture diffusion

Test variables. Experiments on moisture diffusion were performed to determine D_1, the maximum of $D(H)$ for $H=1$ (m^2/s) and f, the surface factor: these are the relevant properties of moisture diffusion of the inner concrete of SRC column specimens.[6,7] Fig. 4 shows the dimensions of the specimens and the measurement locations in the experiments conducted for estimation of moisture diffusion.[4] Two specimens with identical cross-sections (100×100 mm^2) and lengths (200 mm) were manufactured and tested under different exposure conditions to the at-

Table 1. Mix proportions of concrete

Test variables	w/b: %	Fine aggregate ratio: %	Unit weight: kg/m^3						
			Water	Cement	Fly ash	Slag	Fine aggregate	Coarse aggregate	Superplasticiser
C1 (RC)	38·0	48·0	148	273	78	39	836	923	5·46
C2 (SRC)	33·9	43·0	161	403	48	24	720	976	6·65

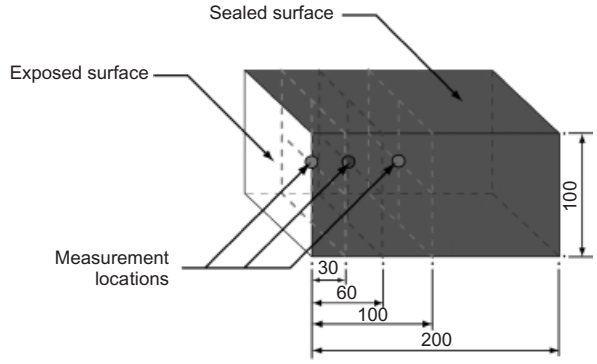

Fig. 4. Dimensions of specimen and locations of moisture diffusion measurement in experiment. Units: mm

mosphere. Two companion specimens for each case were manufactured and tested.

Test set-up. After initial moisture curing for 1 day, the specimens were placed in a constant temperature and constant humidity chamber under conditions of 20 ± 1°C and 60 ± 2% RH.[3] For each set of two specimens, which were exposed to different atmospheric conditions as described in the test variables section, one specimen, (E), was exposed to air through only one surface. The remaining surfaces were sealed with several layers of waterproof plastic film, as shown in Fig. 4, in order to measure the total moisture loss occurring from the interior of the concrete to the atmosphere in one direction only. The other specimen, (S), was sealed with several layers of waterproof plastic film along all the surfaces in order to prevent moisture diffusion from the interior of the concrete to the atmosphere. The pore relative humidity is generally used to represent the moisture conditions of concrete, and it can be measured by relative humidity probes installed in a drilled cavity.[8–10] Relative humidity inside the exposed specimens (E) was measured at distances of 30, 60 and 100 mm from the exposed surface. Relative humidity inside the sealed specimens (S) was measured at the centre of the specimen so as to measure the moisture loss caused by self-desiccation, which was measured to predict moisture loss owing to drying alone.

Materials. The mix proportion of all the specimens corresponds that of the SRC column specimen (C2) in Table 1.

Analytical programme

In this study, finite-element analyses were employed to estimate the moisture diffusion, differential drying shrinkage, and differential stress-induced shrinkage in the test specimens.

Analysis of long-term behaviour of column specimens without consideration of differential moisture distribution

Generally, model codes such as the American Concrete Institute (ACI) and CEB–FIP are used to calculate the column shortening in concrete structures, considering both mix proportion and exposed ambient conditions. These models are used when estimating the long-term deformation of concrete owing to factors such as drying shrinkage and creep. The estimation result depends on the model used.

In this paper, an analysis of the long-term behaviour of column specimens was performed by using the CEB–FIP model code and age-adjusted effective modulus method (AEMM). The notional shrinkage coefficient ε_{cso} and the notional creep coefficient ϕ_0 were determined from regression analyses for controlling tests. Values of ε_{cso} and ϕ_0 for C1 concrete applied to RC column specimens were 576×10^{-6} and 1·91, respectively, while values of ε_{cso} and ϕ_0 for C2 concrete applied to SRC column specimens were 574×10^{-6} and 2·29, respectively. ε_{cso} and ϕ_0 were determined so as to predict the long-term behaviour of column specimens without considering the differential moisture distribution.

Analysis of the progress of moisture diffusion

A regression analysis was performed on the results of experiments on moisture diffusion in order to determine two factors: D_1, the maximum of $D(H)$ for $H = 1$ (m^2/s); and f, the surface factor of concrete C2 applied to SRC column specimens. The specimens exposed to air through only one surface (E) were modelled using the finite-element method. The progress of moisture diffusion through these specimens was calculated using the non-linear moisture diffusion equation, as given in equation (1). A numerical step-by-step procedure at any time t and the Newmark β integration method were used.[11]

$$\frac{\partial H}{\partial t} = \left[\frac{\partial}{\partial x}\left(D\frac{\partial H}{\partial x}\right) + \frac{\partial}{\partial y}\left(D\frac{\partial H}{\partial y}\right) + \frac{\partial}{\partial z}\left(D\frac{\partial H}{\partial z}\right)\right] \tag{1}$$

The Newmark β integration method assumes the following equations

$$\dot{H}^{t+\Delta t} = \dot{H}^t + \left[(1-\delta)\ddot{H}^t + \delta\ddot{H}^{t+\Delta t}\right]\Delta t \tag{2}$$

$$H^{t+\Delta t} = H^t + \dot{H}^t\Delta t + \left[\left(\frac{1}{2}-\beta\right)\ddot{H}^t + \beta\ddot{H}^{t+\Delta t}\right](\Delta t)^2 \tag{3}$$

An analysis of the progress of moisture diffusion through the SRC column specimens was performed in the same manner, that is by using the values of D_1 and f, which were determined from a regression analysis of

the moisture diffusion experiment. The SRC column specimens were modelled using the finite-element method. A steel section was modelled as a barrier to moisture diffusion so as to consider the effect of obstruction of the moisture diffusion route by a steel section. The results of the analysis were applied to the analysis of the long-term behaviour of SRC column specimens with consideration of the differential moisture distribution.

Analysis of long-term behaviour of SRC column specimens with consideration of differential moisture distribution

In previous studies, attempts were made to consider the effect of moisture distribution on concrete structures.[7,12,13] For a given cross-section and length of time, Bazant and co-workers expressed the variation of differential drying shrinkage and the variation of stress-induced shrinkage in terms of the variation of relative humidity, ΔH.[14–16] In the proposed equations, k, one of the most important factors, is expressed as follows

$$k = k_{sh}[1 + r\boldsymbol{\sigma}\, sign(\overline{H})] \tag{4}$$

where r is a constant for shrinkage, $\boldsymbol{\sigma}$ is a stress in a cross-section and $sign(\overline{H})$ is the sign of the microdiffusion flux, $\overline{H}$.

$$k_{sh} = \varepsilon_s^0 g_s(t) \tag{5}$$

$$g_s(t) = E_c(t_0)/E_c(t)$$

$$E_c(t) = E_c(28)\sqrt{\frac{t}{4 + 0{\cdot}85t}}$$

$$E_c(28) = 0{\cdot}043w^{1{\cdot}5}\sqrt{\boldsymbol{f}'_c}$$

where ε_s^0 is the magnitude of the final shrinkage value.

In this paper, r in equation (4) and ε_s^0 in equation (5) are the major variables to be determined by the regression analysis applied to the results of control tests: the variables determined by the regression analysis were $\varepsilon_s^0 = -1000 \times 10^{-6}$ and $r = 1{\cdot}77 \times 10^{-8}$, respectively. r, ε_s^0 and ΔH, which are the outcomes of the analysis on the progress of moisture diffusion through the SRC column specimens, were utilised in order to predict the long-term behaviour of the SRC column specimens with consideration of the differential moisture distribution. The analysis was performed by a numerical step-by-step procedure at any time t.[11]

Results and discussion

Prediction of long-term behaviour of column specimens without consideration of differential moisture distribution

Figure 5 presents a comparison of the results obtained from the analysis of the long-term behaviour of column specimens, without considering the differential moisture distribution, with those obtained from experiments. Fig. 5 indicates that the results for the analysis of the long-term behaviour of RC column specimens (RC1 and RC2) agree reasonably well with the experimental results. For the SRC column specimens (SRC1 and SRC2), however, there is a certain degree of mismatch between the results of the analysis and those of experiments. What then are the factors responsible for this discrepancy in the case of SRC column specimens?

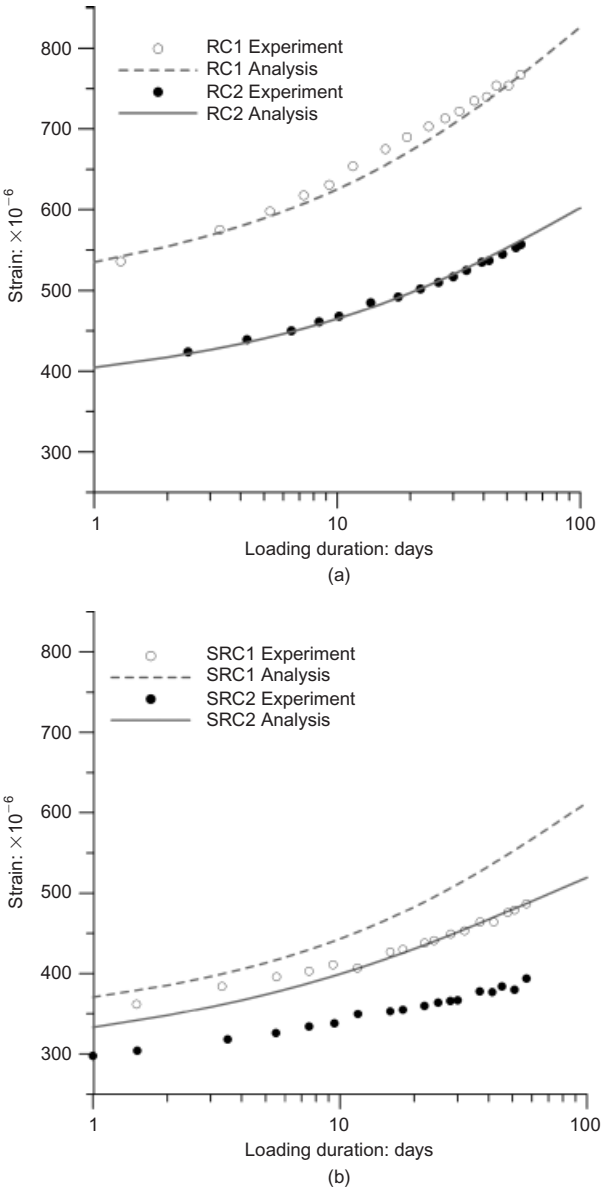

Fig. 5. Comparison between experimental and analysis results without considering the effect of differential moisture distribution: (a) RC1 and RC2; (b) SRC1 and SRC2

In the models proposed by ACI[17] and CEB–FIP,[6] it is assumed that the differential moisture distribution in a given cross-section is the average moisture distribution: this means that the drying shrinkage and the drying creep are equal throughout the entire section.

For example, in the CEB–FIP model code,[6] the progress of drying shrinkage is expressed as a function of h (notional size of member) as follows

$$\beta_s(t-t_s)=\sqrt{\frac{(t-t_s)/t_1}{\beta_{SH}+(t-t_s)/t_1}} \quad (6)$$

where $t_1 = 1$ day, $\beta_{SH} = 350(h/h_0)^2$, $h_0 = 100$ mm, and $h = 2A_c/u$ mm where A_c represents the cross-section and u represents the perimeter of the member in contact with the atmosphere.

The progress of creep is also expressed in terms of h without distinguishing the creep into two types—basic creep and drying creep—in the CEB–FIP model code.[6] As a result, both the drying shrinkage and the drying creep of concrete inside the SRC columns are bound to be overestimated since the unique property of moisture diffusion in the SRC columns cannot be considered in terms of h alone when using this model code. In other words, owing to this overestimation of drying creep and drying shrinkage, the effect of the obstruction of the moisture diffusion route by the steel section, as shown in Fig. 1, cannot be taken into account. Overestimation of drying shrinkage and drying creep of concrete inside the SRC columns may also occur when using the ACI model. The ACI model[17] expresses the progress of drying shrinkage and drying creep as a function of v/s (volume/surface area) and ignores the differential moisture distribution. Overestimation of SRC column shortening will therefore inevitably result from the use of any of the existing prediction models, since none of them considers the effect of the obstruction of the moisture diffusion route by the steel section.

Prediction of the progress of moisture diffusion

Figure 6 shows the results of the regression analysis applied to the results of experiments conducted on moisture diffusion. From the results of the regression analysis the values of D_1 and f of concrete C2 applied to SRC column specimens were determined: $D_1 = 1{\cdot}8 \times 10^{-6}$ m^2/h and $f = 12 \times 10^{-6}$ m/h; these values were thereupon applied to the moisture diffusion analysis of the SRC column specimens.

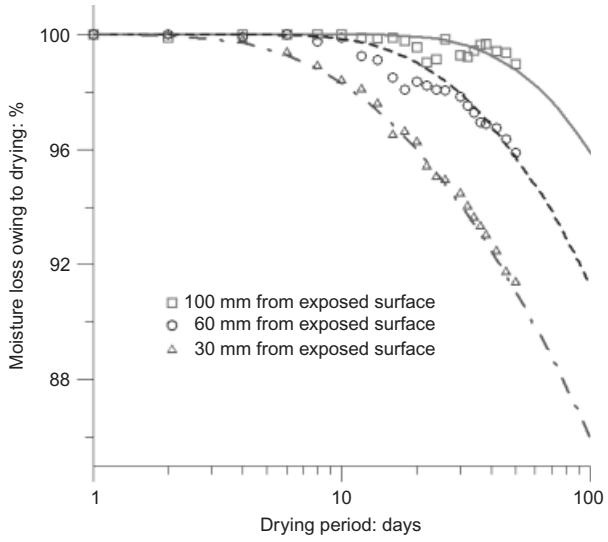

Fig. 6. Result of regression analysis on moisture diffusion

Figure 7 shows the results of the analysis on the progress of moisture diffusion of SRC1 alongside those for an RC column with the same cross-section and mix proportion. The RC column was modelled as a plain concrete column by ignoring the effect of bars obstructing the moisture diffusion route. As shown in Fig. 7, moisture diffusion inside the steel section in the SRC column occurs slower than that inside the RC column since the steel section (such as an H-shaped steel section) obstructs the moisture diffusion route of the inner concrete: this may lead to relatively lesser shortening of the SRC column relative to the RC column. In addition, moisture diffusion outside the steel flange section in the SRC column progresses relatively faster compared to that of the RC column; this may lead to the appearance of additional cracks in the steel flange side of the SRC column relative to those in an RC column. These analytical results were applied to the analysis of the long-term behaviour of SRC column specimens with consideration of the differential moisture distribution to calculate both the differential drying shrinkage and the differential stress-induced shrinkage in terms of ΔH.

Prediction of long-term behaviour of SRC column specimens with consideration of differential moisture distribution

A prediction of the long-term behaviour of SRC column specimens with consideration of the differential moisture distribution was carried out. The results of the analysis of the progress of moisture diffusion of SRC column specimens and the regression analysis of the results of control tests ($\varepsilon_s^0 = -1000 \times 10^{-6}$ and $r = 1{\cdot}77 \times 10^{-8}$) were used. Fig. 8 provides a comparison of the results of the analysis on long-term behaviour of SRC1 with those of the experiment for the cases of considering and ignoring the differential moisture distribution. It is evident from Fig. 8 that the analysis method that incorporates consideration of the differential moisture distribution is relatively more accurate than that which disregards the differential moisture distribution. Therefore, in order to predict the shortening of SRC columns more accurately, the differential moisture distribution, caused by obstruction of the moisture diffusion route, should be taken into account in the column shortening analysis.

Discussion on practical application of proposed approach

The progress of moisture diffusion in SRC columns is vastly different from that in RC columns owing to the obstruction of the moisture diffusion route caused by a steel section. This may induce a reduction in both

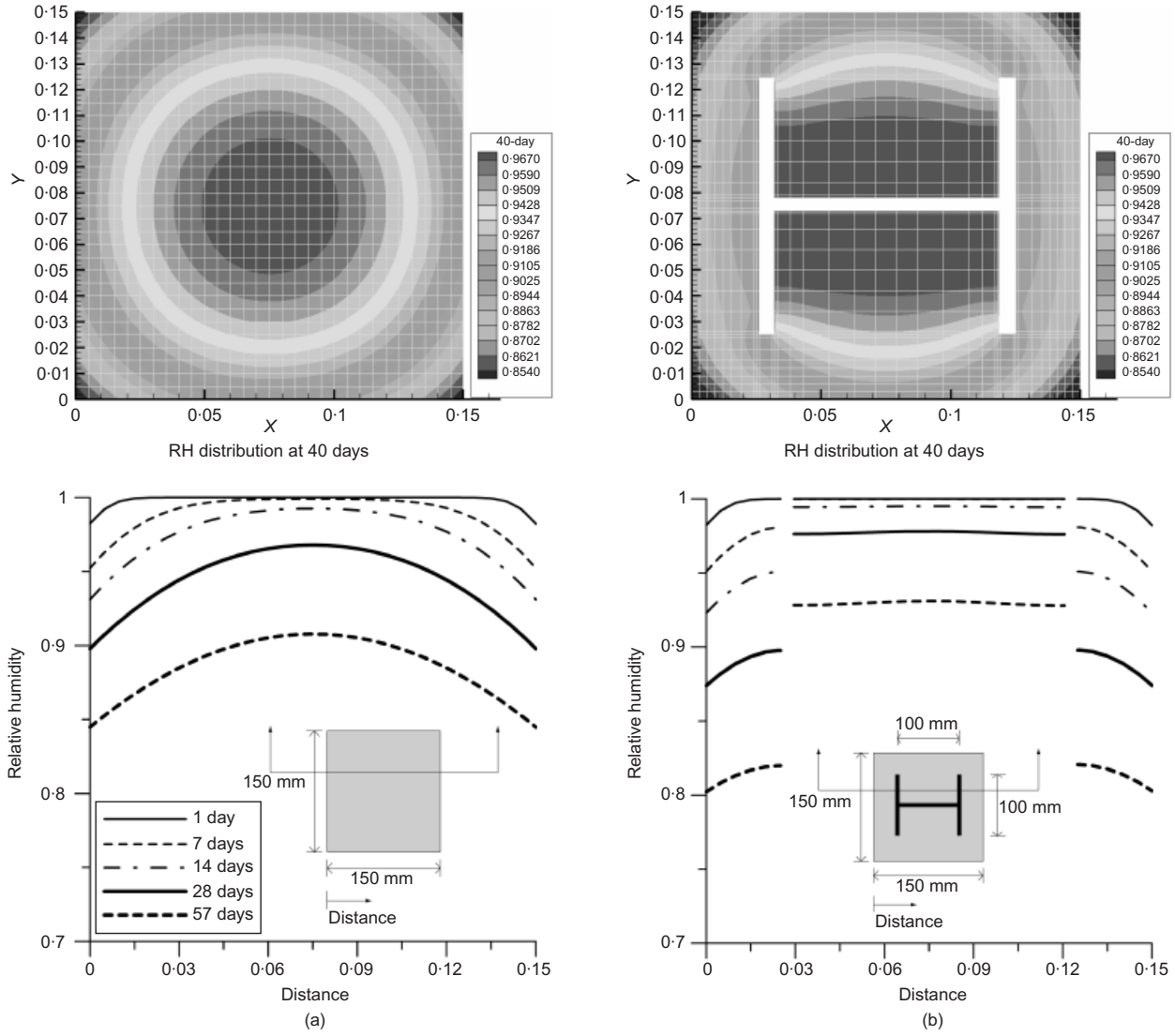

Fig. 7. Result of analysis on the progress of moisture diffusion: (a) RH distribution of RC column; (b) RH distribution of SRC column

drying shrinkage and drying creep in the case of SRC columns.

These obtained results have been applied to modified versions of shrinkage and creep equations in the CEB–FIP model code[6] with the goal of predicting the shortening of SRC columns more accurately. It is assumed that the notional shrinkage coefficient ε_{cso} and the notional creep coefficient ϕ_0 are constant, regardless of the dimensions of the column, and the differences between RC and SRC column behaviour are caused by only the moisture diffusion characteristic. In the CEB–FIP model code, the progress of drying shrinkage at any time t is expressed as a function of $\beta_s(t - t_s)$, as shown in equation (6). The progress of drying creep at any time t is expressed as a function of $\beta_c(t - t_0)$. $\beta_s(t - t_s)$ and $\beta_c(t - t_0)$ were modified as shown in equation (7) and equation (8) so as to consider the differential moisture distribution in SRC columns: the target variables to be determined by the analysis were α and γ.

$$\beta_s(t - t_s) = \sqrt{\frac{(t - t_s)/t_1}{\beta_{SH} + (t - t_s)/t_1}} \quad \rightarrow \quad \beta'_s(t - t_s) = \sqrt{\frac{(t - t_s)/t_1}{\alpha\beta_{SH} + (t - t_s)/t_1}} \tag{7}$$

$$\beta_c(t - t_0) = \left[\frac{(t - t_0)/t_1}{\beta_H + (t - t_0)/t_1}\right]^{0\cdot3} \quad \rightarrow \quad \beta'_c(t - t_0) = \left[\frac{(t - t_0)/t_1}{\gamma\beta_H + (t - t_0)/t_1}\right]^{0\cdot3} \tag{8}$$

The dimensions of the columns, as shown in Fig. 9, and the mix proportion of concrete C2, as shown in Table 1, were used for modification of the CEB–FIP model code. It was assumed that the stiffness of a steel section, $\boldsymbol{EA}$, had a zero value and its thickness was negligible in order to consider the effects of the differential moisture distribution only. It is therefore expected that the long-term behaviour of a plain concrete

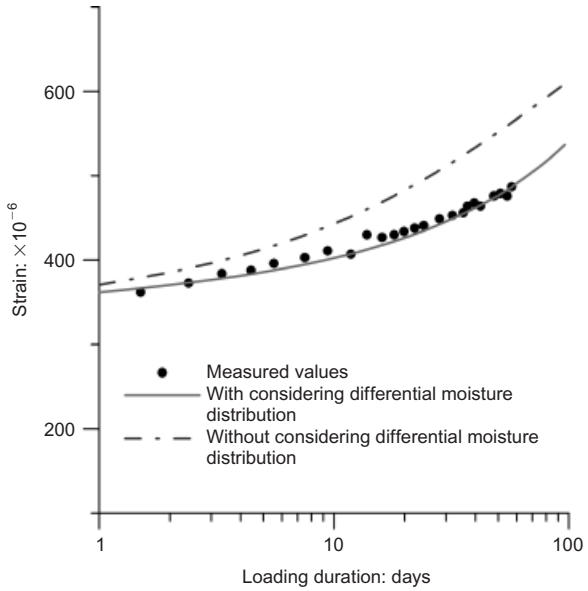

Fig. 8. Comparison between experimental and analysis results for SRC1 column specimen with consideration of the effect of differential moisture distribution

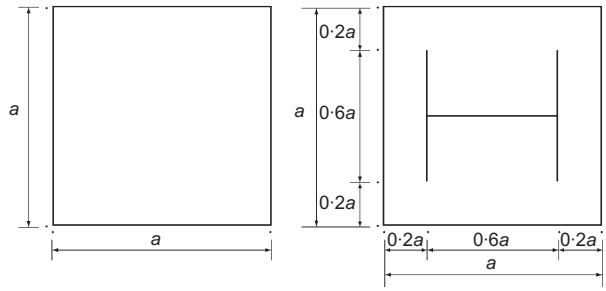

Fig. 9. Dimensions of columns for analysis. a = 500, 800, 1000 mm

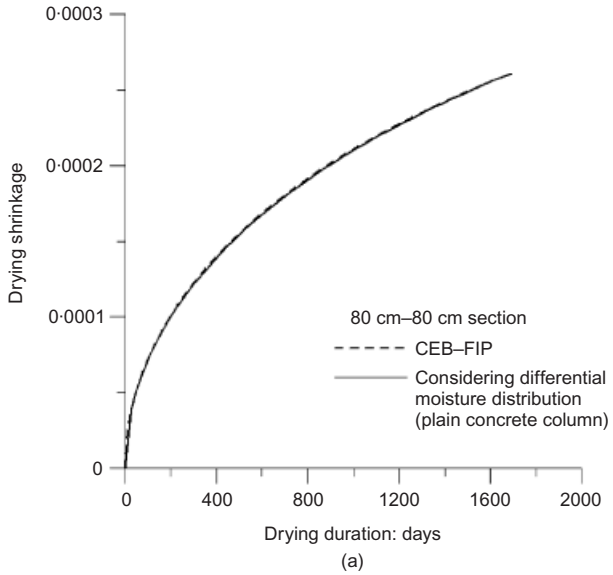

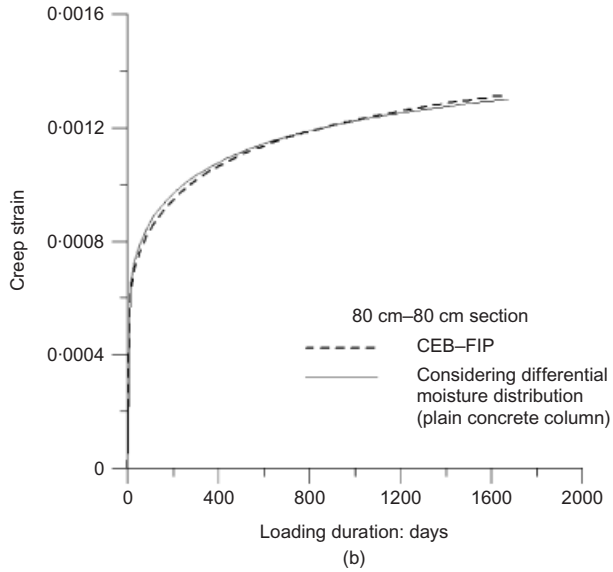

Fig. 10. Long-term behaviour of plain concrete column with consideration of differential moisture distribution: (a) drying shrinkage; (b) creep

column will be nearly the same as that of an SRC column while using the CEB–FIP model code. First, variables such as ε_s^0 and r were adjusted so that the long-term behaviour of plain concrete column will correspond with the predicted behaviour using the CEB–FIP model code, as shown Fig. 10.

An analysis was performed on the long-term behaviour of SRC columns with adjusted variables, as shown in Fig. 11: this analysis was denoted as analysis-A. It is evident from Fig. 11 that there is a certain degree of mismatch between the long-term behaviour of the SRC column and that evaluated by the CEB–FIP model code. The values of α and γ, as given in Table 3, were determined such that the results of analysis A and the CEB–FIP model code with both $\beta_s'(t - t_s)$ and $\beta_c'(t - t_0)$ functions would agree. Values of α are relatively constant as compared to the decrease of γ values with an increase of the A_c/u ratio, where A_c represents the cross-section and u represents the perimeter of the member in contact with the atmosphere. Hence, the values of α can be suggested as an average value, and the γ value can be expressed as a function of the A_c/u ratio.

$$\alpha = 1{\cdot}2 \tag{9}$$

$$\gamma = -0{\cdot}006(A_c/u) + 2{\cdot}85 \tag{10}$$

The practical application presented in this section was performed as an example of the proposed approach. Since $\beta_s'(t - t_s)$ and $\beta_c'(t - t_0)$ are based on certain limited assumptions such as limited dimensions of columns and limited mix proportions, the variables α and γ may have different values according to the applied assumptions. Therefore, more rigorous analyses are needed in order to propose a more generalised modification.

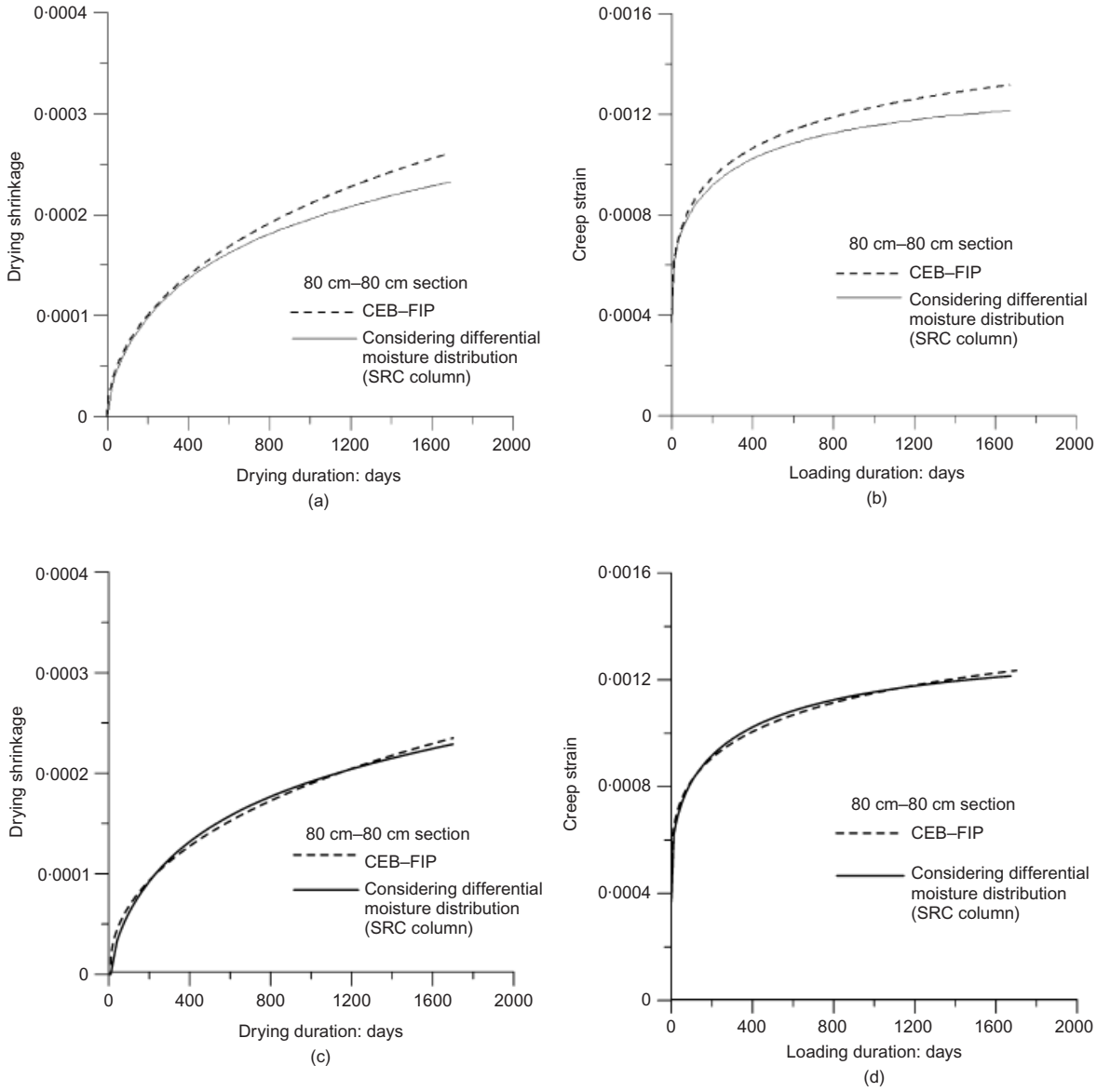

Fig. 11. Long-term behaviour of SRC column with consideration of differential moisture distribution: (a) drying shrinkage (before modification); (b) creep (before modification); (c) drying shrinkage (after modification); (d) creep (after modification)

Table 3. α and γ determined from the regression analysis

Dimension of columns: mm × mm	A_c/u: mm	α	γ
500 × 500	125	1·185	2·150
800 × 800	200	1·193	1·643
1000 × 1000	250	1·188	1·442

Conclusions

In this study, the differential moisture distribution caused by obstruction of the moisture diffusion route in SRC columns has been investigated with the aim of demonstrating its importance with respect to the accurate prediction of the shortening of SRC columns. From the results of this investigation, the following conclusions can be drawn.

(*a*) The progress of moisture diffusion in SRC columns is different from that of RC columns, since a steel section obstructs the moisture diffusion route of the inner concrete in SRC columns.
(*b*) Differential moisture distribution caused by obstruction of the moisture diffusion route affects both drying shrinkage and drying creep in SRC columns.
(*c*) Overestimation of steel-reinforced concrete column shortening is bound to occur while using the existing prediction models, all of which exclude the effects of the differential moisture distribution.
(*d*) A more accurate prediction method of SRC column shortening has been proposed. The proposed

approach incorporates the differential moisture distribution in SRC columns, which is caused by obstruction of the moisture diffusion route and is found to affect both drying shrinkage and drying creep.

Acknowledgement

The authors would like to thank the Infra-Structures Assessment Research Center (ISARC) funded by the Korea Ministry of Construction and Transportation (MOCT) for financial support.

References

1. Ghosh M. F. and Iyengar H. *Column Shortening in Tall Structures: Prediction and Compensation.* Portland Cement Association, Skokie, IL, USA, 1987, Engineering Bulletine No. EB10 8D, pp. 34.
2. Elimerie M. M. and Joglekar M. R. *ACI SP-117: Influence of Column Shortening in Reinforced Concrete and Composite High-rise Structures*. American Concrete Institute, Detroit, 1989, pp. 55-86.
3. Kwon S. H., Kim J. K. and Jung H. W. Experimental study on long-term behaviour of RC and SRC Columns. *Proceedings of the Korea Concrete Institute,* 2003, **15**, No. 1, 481–486 (in Korean).
4. Seol H. C., Kim Y. Y., Kwon S. H., Kim H. S. and Kim J. K. Column shortening of SRC columns considering the differential moisture distribution. *Journal of KCI*, 2006, **18**, No. 1, 29–36 (in Korean).
5. Hyundai Institute of Construction Technology. *A Study on Column Shortening of Composite Column in Tall Buildings*, Hyundai Institute of Construction Technology, Seoul, Korea, 2004.
6. Comité Euro-International Du Béton. *CEB–FIP Model Code 1990*. Thomas Telford, London, 1993.
7. Sakata K. A study on moisture diffusion in drying and drying shrinkage of concrete. *Cement and Concrete Research*, 1983, **13**, No. 2, 216–224.
8. Parrot L. J. Factors influencing relative humidity in concrete. *Magazine of Concrete Research*, 1991, **43**, No. 154, 45–52.
9. Terrill J. M., Richardson M. and Selby A. R. Non-linear moisture profiles and shrinkage in concrete members. *Magazine of Concrete Research*, 1986, **38**, No. 137, 220–225.
10. Merikallio T., Mannonen R. and Penttala V. Drying of lightweight concrete produced from crushed expanded clay aggregate. *Cement and Concrete Research*, 1996, **26**, No. 9, 1423–1433.
11. Kim J. K. and Lee C. S. Prediction of differential drying shrinkage in concrete. *Cement and Concrete Research*, 1998, **28**, No. 7, 985–994.
12. Bazant Z. P. and Thonguthai W. Pore pressure and drying of concrete at high temperature. *Journal of Engineering Mechanics Division, ASCE*, 1978, **104**, No. EM5, 1059–1079.
13. Illston J. M. and Tajirian A. Computer experiments on environmentally induced stresses in unreinforced concrete pavement slabs. *Magazine of Concrete Research*, 1977, **29**, No. 101, 175–190.
14. Bazant Z. P. and Yunping X. Drying creep of concrete: constitutive model and new experiments separating its mechanisms. *Materials and Structures*, 1994, **27**, No. 1, 3–14.
15. Bazant Z. P. and Raftshol W. J. Effect of cracking in drying and shrinkage specimens. *Cement and Concrete Research*, 1982, **12**, No. 2, 209–226.
16. Bazant Z. P., Kristek V. and Vitek J. Drying and cracking effects in box-girder bridge segment. *Journal of Structural Engineering, ASCE*, 1992, **118**, No. 1, 305–321.
17. American Concrete Institute. *Prediction of Creep, Shrinkage and Temperature Effects in Concrete Structures.* ACI, Detroit, 1992, ACI Committee 209, ACI 209 R-92.

Discussion contributions on this paper should reach the editor by 1 December 2008